

A promising approach for lithium iron phosphate (LFP) battery black mass recycling for fertilizer production

Downloaded from: https://research.chalmers.se, 2026-11-20 08:32 UTC

Citation for the original published paper (version of record):

Segura Bailon, B., Miksovsky, P., Ebin, B. et al (2027). A promising approach for lithium iron phosphate (LFP) battery black mass recycling for fertilizer production. Resources, Conservation and Recycling, 238. http://dx.doi.org/10.1016/j.resconrec.2026.109219

N.B. When citing this work, cite the original published paper.

research.chalmers.se offers the possibility of retrieving research publications produced at Chalmers University of Technology. It covers all kind of research output: articles, dissertations, conference papers, reports etc. since 2004. research.chalmers.se is administrated and maintained by Chalmers Library

(article starts on next page)

Resources, Conservation & Recycling 238 (2027) 109219

Contents lists available at ScienceDirect

Resources, Conservation & Recycling

journal homepage: www.sciencedirect.com/journal/resources-conservation-and-recycling

A promising approach for lithium iron phosphate (LFP) battery black mass recycling for fertilizer production

Brenda Segura-Bailón *, Philipp Mikšovsky, Burçak Ebin, Martina Petranikova

Department of Chemistry and Chemical Engineering, Industrial Materials Recycling and Nuclear Chemistry, Chalmers University of Technology, Gothenburg, Sweden

ARTICLE INFO

Keywords:
Spent lithium-ion batteries
Fertilizer production
Selective leaching
Base metal extraction
Lithium recovery

ABSTRACT

The manufacture of agricultural products has recently gained attention, particularly in the search for practical methods to replace traditional mineral-based raw materials. Therefore, this investigation presents an innovative hydrometallurgical process for producing fertilizers from spent lithium-iron phosphate batteries. Additionally, this work developed a method to produce lithium phosphate as a subproduct. To extract lithium, sodium hydroxide (NaOH) was used; with 2 M NaOH, 20 g/L, 60 min at 25 °C, 98% of lithium was dissolved. Lithium phosphate (purity >98%) was then obtained by precipitation. The solid residue from the alkaline leaching was treated with ethylenediaminetetraacetic acid (EDTA). 98% Fe and ~96% Cu were extracted (0.3 M EDTA, 60 °C,120 min); therefore, these leachates are promising for fertilizer production. Furthermore, the content of electrolyte solvents and fluoride was analyzed. Electrolyte solvents decomposed in alkaline media, and fluoride concentration was significantly lower than levels found in natural soils, yielding products free of impurities.

1. Introduction

1.1. Challenges in agricultural product manufacturing for food security

According to the European Union (EU), sustainable agriculture entails practices and methods that achieve four primary objectives: mitigating climate change, efficient management of natural resources, protecting biodiversity, and promoting animal welfare (European Commission: Sustainable agriculture in the EU, 2025). Hence, many efforts have been focused on creating new strategies to ensure global food security. One of them is the production of more environmentally friendly products, such as fertilizers and pesticides (herbicides, insecticides, and fungicides).

Traditionally, minerals are the primary raw material for fertilizer production; nevertheless, the shortages of ore, geography and geopolitical factors, as well as greenhouse gas emissions, are directly related to fertilizer supply (Quitzow et al., 2025). To meet the current market demand for fertilizers, which is expected to grow from USD 230.10 billion in 2025 to USD 281.56 billion by 2030 (Markets and markets: Fertilizers Market by Type (Chemical Fertilizers and Biofertilizers), 2025), new technologies have been developed, including nano and biofertilizer manufacturing. These advancements use live formulations in which microorganisms enhance nutrient availability to plants, thereby promoting biosafety in agriculture; however, these methods are still under investigation (Gehlot et al., 2024; Zulfiqar et al., 2025). On the other hand, recycled raw materials have emerged as a sustainable method for creating new products. In this context, battery recycling is an alternative for fertilizer production (Zhou et al., 2024). Lithium-ion batteries (LIBs) contain valuable elements such as lithium, cobalt, nickel, manganese, copper, iron, aluminum, phosphorus, etc., which can be recovered and used as nutrients for plant health and growth (Hazra, 2016; Zhou et al., 2024).

1.2. Battery recycling focused on fertilizer production

Fertilizer production from spent batteries is a relatively unexplored area of research. Some published works have examined the treatment of alkaline, nickel-cobalt-manganese (NMC), and lithium-iron phosphate ($LiFePO_4$, LFP) batteries. Most of these studies focus on the formulation of nitrogen, phosphorus, and potassium compounds, as these three elements are commonly found in commercial fertilizers (Hazra, 2016). For example, Fazilova et al. (2023) studied how cathode material from NMC batteries can be used as a polymicroelement-containing additive to enhance the properties of ammonium nitrate (NH_4NO_3). In this work, introducing lithium powders into the ammonium nitrate melt (175 °C) increased the amount of microelements such as lithium (0.0094% to

* Corresponding author.
E-mail address: bailon@chalmers.se (B. Segura-Bailón).

https://doi.org/10.1016/j.resconrec.2026.109219
Received 2 June 2026; Received in revised form 15 October 2026; Accepted 26 October 2026
Available online 30 October 2026
0921-3449/© 2026 The Author(s). Published by Elsevier B.V. This is an open access article under the CC BY license (http://creativecommons.org/licenses/by/4.0/).

0.0527%), cobalt (0.0561% to 0.2395%), manganese (0.0387% to 0.2860%), and nickel (0.0112% to 0.0387%). This process allows to replace the use of pure salts and reduce cost in the production of this type of fertilizer. However, the energy consumption during the melting process needs to be analyzed to assess the feasibility of the process.

On the other hand, hydrometallurgical techniques have also been used to process spent batteries and produce fertilizers. These methods have been shown to efficiently dissolve metals in short reaction times and promote selectivity (Li et al., 2024). Selectivity is crucial for effectively processing complex materials, especially when specific components are required for particular applications. Based on these principles, Yue et al. (2021) suggested a methodology to recover phosphorus and lithium from cathode active material from LFP batteries. A multi-step process was carried out. First, the active cathode material was separated from the aluminum foil using 0.4 M sodium hydroxide (NaOH) under ultrasound for 15 min. Then, the cathode power was treated in sodium persulfate solutions ($Na_2S_2O_8$) for lithium dissolution. ≥99.5% Li was extracted under the experimental conditions: 2:1.4 mol/mol $Na_2S_2O_8$, 50 g/L, 30 min, at 25 °C. Subsequently, the delithiated cathode material was leached in sodium sulfide ($Na_2S{\cdot}9H_2O$) to dissolve phosphate. In this stage, parameters such as solid-liquid ratio (2.5–100 g/L), leaching time (0.5- 5 h), and $Na_2S{\cdot}9H_2O$ concentration (1–1:2.5 mol/mol) were analyzed. After this leaching stage, the pH of the solutions was adjusted with phosphoric acid (H_3PO_4). As the last step, a phosphorus-grafted slow-release fertilizer (P-SRF) was prepared by adding urea, methylbutandionic acid (MBA), and potassium persulfate (KPS) to phosphate solutions.

Another hydrometallurgical route was proposed by Zhang et al. (2023), who implemented a process for LFP cathode material treatment using organic and inorganic compounds, where citric ($C_6H_8O_7$), oxalic ($C_2H_2O_4$), and sulfuric (H_2SO_4) acid were tested. The main objective of these leaching agents was to recover lithium and use the residual leachates as fertilizers. Oxalic acid (experimental conditions: 0.5 $C_2H_2O_4$, 50 g/L, 80 °C, 60 min, 300 rpm) allowed 95% lithium extraction, while iron was extracted <5%. Afterward, the leaching solutions, which were rich in lithium and phosphate ions, were processed through ion-exchange resins (K-form, K350). This process allowed the binding of lithium to the resins and the release of potassium into the phosphate solutions. As a result, solutions rich in potassium and phosphate ions (K^+, PO_4^{3-}) were obtained, making them suitable for use as fertilizers. The authors affirmed that the use of K-form ion-exchange resins is a low-cost and conventional method for treating LFP cathode material, providing a new approach to the use of resins in battery recycling.

Finally, Barragán-Mantilla et al. (2024) developed a process to recover zinc and manganese from alkaline zinc carbon-based batteries, which contain a high amount of zinc and manganese (25.45 wt% Zn and 37.89 wt% Mn). Sulfuric acid (H_2SO_4), citric acid ($C_6H_8O_7$), and glycine ($C_2H_5NO_2$, gly) were studied and compared. Different concentrations of leaching agents (0.25, 0.5, and 1 M) were tested, and a solid-liquid ratio of 100 g/L was employed. The experiments were carried out at 25 °C and 60 °C, and acidic and alkaline media were analyzed. Leaching efficiencies of 74%−83% for Zn and Mn were obtained, especially in citrate and glycine solutions, in the pH range from 6 to 7. This work determined that leachates with Zn-Mn-citrate and Zn-Mn-gly complexes are potential fertilizers. Nowadays, alkaline battery treatment for fertilizer production is considered a feasible technology. ReNutrients, an Australian company, processes black mass from alkaline batteries and offers fertilizers enriched with zinc and manganese (ReNutrients, 2025).

The outlined methodologies provide an overview of how agricultural products can be manufactured from spent batteries, emphasizing the importance of battery recycling. Nevertheless, studies are needed to evaluate the potential of combined methodologies to recover both valuable and less valuable metals, while effectively utilizing the entire sample. Additionally, analyzing the behavior of non-metallic substances in leachates (e.g., decomposition products of electrolyte and binder) is not addressed. This information could provide insights into their use in manufacturing agricultural products.

The methodologies described also highlight the need to research the processing of low-value materials, for example, LFP batteries. This type of battery is currently experiencing significant production growth, with the market projected to grow from USD 30.36 billion in 2026 to USD 77.07 billion by 2034 (Fortune Business Insights: Lithium Iron Phosphate Battery Market Size, Share & Industry Analysis, 2025). The reasons include low cost, low fire risk, and a chemical composition free of cobalt, nickel, rare earth elements, and other toxic materials (Luo et al., 2025). For recycling purposes, lithium is perhaps the most valuable metal to recover, but other metallic components should also be recycled, considering environmental and circular economy reasons. Moreover, LFP recycling is economically viable compared with recycling other battery chemistries (Zhao et al., 2024).

As an innovative alternative, this work proposes a hydrometallurgical process for treating LFP black mass. The aim is to recover iron and reincorporate it into the market for fertilizer production. This metal represents between 35 and 43 wt% of the active material in an LFP battery (Wang et al., 2016; Passalacqua, 2023). Furthermore, iron is classified as a micronutrient responsible for plant growth and productivity, and is implicated in biological processes such as photosynthesis and chlorophyll biosynthesis (Liu et al., 2022; Anka et al., 2023; Alzate-Zuluaga et al., 2023). So, iron recycling is a profitable source for generating agricultural products.

Due to the LFP battery chemistry, it is also possible to recover lithium and phosphorus and use them as raw materials to produce new lithium-ion batteries. Therefore, the proposed methodology involves two-stage leaching and a recovery stage (Fig. 1). Firstly, alkaline leaching using sodium hydroxide (NaOH) solutions is proposed to selectively extract lithium. Afterward, lithium is recovered from the Pregnant Leach Solutions (PLS) by precipitation to produce lithium phosphate salt ($Li_3PO_{4(s)}$). A second leaching phase is suggested to treat solid residues (from the NaOH process) using ethylenediaminetetraacetic acid (EDTA) to dissolve base metals, specifically iron. EDTA was selected because it is a hexadentate chelating ligand, widely used as a sequestering agent, and is thermodynamically stable with some metallic ions found in batteries (e.g., iron, copper, manganese). This compound has also been used in the manufacture of synthetic iron fertilizers, also known as chelated fertilizers (Wolf and Gilbert, 1992; Kasozi et al., 2019; Liu et al., 2022).

To determine the optimal experimental conditions for inorganic (with NaOH) and organic leaching (with EDTA), parameters such as reagent concentration, temperature, and solid-liquid ratio were evaluated. In addition, this study is supported by a thermodynamic analysis that assesses the viability and limitations of each proposed chemical system. The final phase of the proposed methodology focuses on analyzing impurities in leachates, such as electrolyte solvents and fluoride.

2. Materials and methods

2.1. Chemical analysis

A sample of black mass containing approximately 42 wt% graphite, provided by Stena Recycling AB in Sweden, was chemically analyzed to determine its metallic content. The black mass was used without further pretreatment and 0.1 g of sample was digested (in triplicate) in aqua regia prepared with hydrochloric acid (HCl, 37%, Sigma-Aldrich) and nitric acid (HNO_3, 65–67%, Sigma-Aldrich) (HCl: HNO_3 3:1 v/v) at 80 °C, 5 h, and 200 rpm (magnetic agitation). The solutions were cooled,

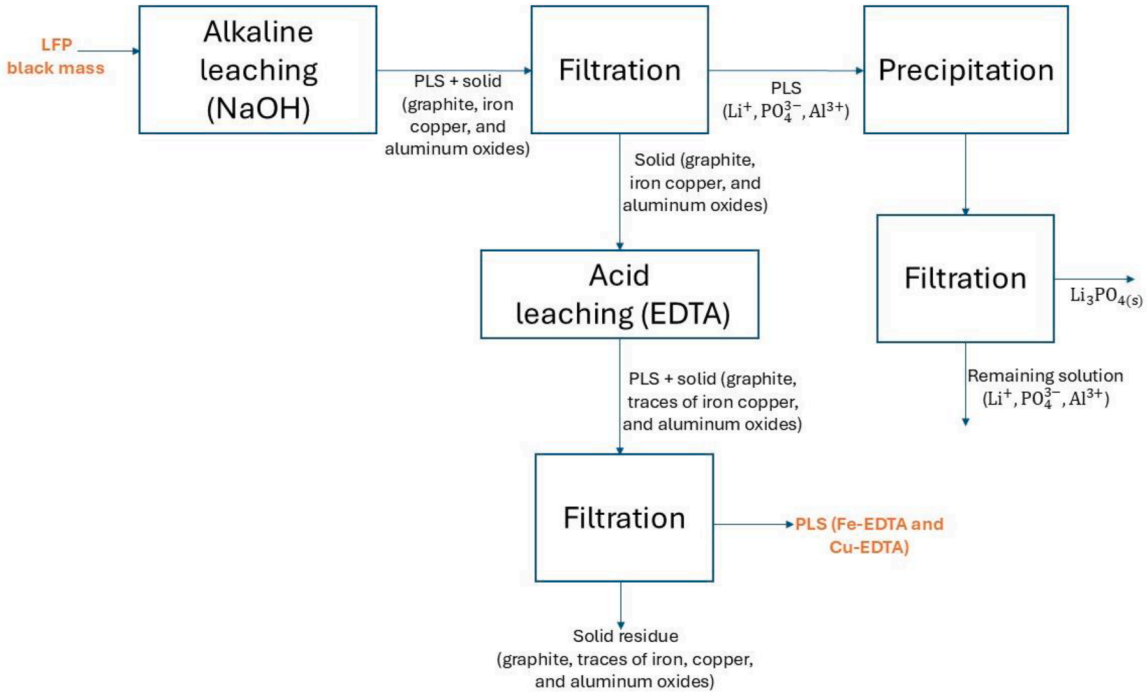


Fig. 1. Flowchart of the proposed methodology.

filtered, and diluted to 100 mL with 0.1 M HNO_3 (65–67%, Sigma-Aldrich). To determine the chemical composition, all samples were analyzed using Inductively Coupled Plasma Optical Emission Spectroscopy (ICP-OES, Thermo Fisher Scientific, Model iCAP™ 6000 Series), and analytical standards (inorganic ventures™) were used to construct the calibration curves.

2.2. Alkaline leaching tests

The black mass sample (without any further physical or chemical pretreatment) was leached with sodium hydroxide (NaOH, ≥98% Sigma-Aldrich) solutions prepared using deionized water (Millipore Milli-Q). The experimental tests, in triplicate, were performed at room temperature (25 °C) using a polypropylene reactor (100 mL, Pyrex) and magnetic agitation (300 rpm). Different concentrations of sodium hydroxide (1, 2, and 4 M) and solid-liquid ratios (20, 40, 60, 80, and 100 g of solid per liter of solution) were tested. Once the leaching process was completed, the solutions were vacuum-filtered, the pH was measured using a MeterLab (PHM240), and analyzed by ICP-OES (Thermo Fisher Scientific, Model iCAP™ 6000 Series). The solid residues were air-dried and subsequently leached in acidic media.

2.3. Acid leaching tests

Ethylenediaminetetraacetic acid (EDTA, >99%, Fluka™) solutions of 0.1 M and 0.3 M (prepared using deionized water, Millipore Milli-Q) were used to leach the solid residues (from the alkaline leaching). All experimental tests (in triplicate) were performed in a double-walled glass reactor (120 mL, Pyrex), with magnetic agitation (300 rpm) at 25 °C, 40 °C, and 60 °C. To control the temperature, a heating circulator (CORIO CP-BC4) was used. Afterward, the solutions were vacuum-filtered, the solid residues were air-dried, digested in aqua regia, and analyzed by ICP-OES to complete the metallurgical balances. The leaching yield (%) was calculated according to Eq. (1). Finally, the pH of the leaching liquors was measured using a MeterLab (PHM240) electrode.

$$\text{Leaching yield } (\%) = \frac{(m_{\text{extracted metal}})}{(m_{\text{extracted metal}}) + (m_{\text{solid residue}})} * 100 \quad (1)$$

2.4. Precipitation process: lithium recovery

Pregnant Leach Solutions (PLS) from alkaline leaching were heated up to 90 °C for 3 h, at 400 rpm based on the methodology proposed by Yang et al. (2024). The experiments were conducted in a double-walled glass reactor (120 mL, Pyrex), using a heating circulator (CORIO CP-BC4) for temperature control. Afterward, the solutions (cooled down to room temperature) were vacuum-filtered, and the solid formed was dried in an oven (Binder FD-23) at 60 °C for 48 h.

2.5. Solid characterization

The solid compound obtained by precipitation was analyzed using X-Ray Diffraction (XRD). A Siemens XRPD diffractometer was utilized, operating with a radiation source in a 2θ interval of 10–80° (Cu λ = 1.54 Å). The instrument was set to a rotational speed of 15 rpm, a voltage of 40 mA, and 40 kV. For the analytical interpretation, EVA Software and the JCPDS database were employed.

2.6. Analysis of residual electrolyte solvents in the black mass, leaching liquors, and solid residue

Gas Chromatography Mass Spectrometry (GC/MS, Agilent Technologies 7890A GC system, 5977A MSD) was performed to analyze the residual electrolyte solvents (ethylene carbonate (EC) and propylene carbonate (PC)) in the original sample, the leaching liquors, and the solid residue, respectively. A capillary column (Agilent, HP-5MS, 30 m x 250 μm x 0.25 μm) was used for the separation (conditions GC: 1 μL injection volume, split ratio: 20:1, 1 mL /min flow of helium, initial temperature: 40 °C, 1 min hold time, ramp 1: 3 °C/min, to 60 °C, ramp 2: 20 °C/min, to 270 °C, hold time: 5 min; conditions MS: EI, temperature MS source 230 °C, solvent delay 2.20 min, 30–500 *m/z*, 5.8 scans/s). For quantification, 0.1 g of black mass was suspended in 10 mL of dichloromethane (CH_2Cl_2). This treatment was performed in triplicate.

After 10 min of treatment in the ultrasound bath at 40 °C, the suspension was filtered (PTFE, 0.45 μm, with prefilter, Thermo Fisher Scientific) through a syringe. A mixture of 0.98 mL of the filtrate and 0.02 mL of the internal standard (20 mg decane/mL dichloromethane) was subjected to GC/MS analysis. A calibration curve was prepared (0.016, 0.031, 0.063, 0.125, 0.25, 0.5, 1.0 mg/mL, internal standard: decane ($C_{10}H_{22}$), 0.4 mg/mL). The limit of detection was 0.002 mg/mL.

For the analysis of the leaching solutions, 5 mL alkaline (2 M NaOH) or acidic (0.3 M EDTA) leaching solution was extracted with 3 mL of dichloromethane. A mixture of 0.98 mL of the organic phase and 0.02 mL of the internal standard (20 mg decane /mL dichloromethane) was subjected to GC/MS analysis.

The analysis of the solid residue was performed using 0.1 g of the solid material, which was suspended in 1.5 mL of dichloromethane. After 10 min treatment in the ultrasound bath at 40 °C, the suspension was filtered (PTFE, 0.45 μm, with prefilter, Thermo Fisher Scientific) through a syringe. A mixture of 0.98 mL of the filtrate and 0.02 mL internal standard (20 mg decane /mL dichloromethane) was subjected to GC/MS analysis.

Finally, the suspensions of black mass were analyzed employing 0.1 g of the solid material, which was suspended in 5 mL of solvent (H_2O, 2 M NaOH or 0.3 M EDTA). After treatment, the suspension was filtered (PTFE, 0.45 μm, with prefilter, Thermo Fisher Scientific) through a syringe. The filtrate was extracted with dichloromethane (2 × 1.5 mL), and the organic phase was analyzed via GC/MS

2.7. Analysis of fluoride in the leaching liquors by a fluoride-selective electrode

The fluoride ion (F^-) content was analyzed potentiometrically using the High-end Titrator for Potentiometric Titration (905 Titrando-Metrohm), a fluoride-selective electrode (Metrohm, model 6.0502.150), and a silver/silver chloride (Ag/AgCl) reference electrode (Metrohm, model 6.0750.100). The liquors were analyzed by adding them in a 1:1 v/v ratio to the ion-strength adjustment buffer concentrate (TISAB IV, Sigma-Aldrich) in polyethylene beakers.

In this study, the leaching liquors from the alkaline medium were diluted (dilution factor of 100) to prevent damage to the electrode membrane and help maintain pH stability. However, the results were calculated taking the dilution factor into account. The pH was measured to ensure a value between 5 and 5.5, and then the fluoride-selective electrode technique was performed. All experiments were conducted in triplicate, and the calibration curve (0.5, 1.0, 2.5, 5, and 10 ppm) was constructed using an analytical standard for ion-selective electrodes (fluoride F^-, Sigma-Aldrich).

2.8. Thermodynamic analysis: species distribution diagrams construction

To analyze the thermodynamic interactions between the organic compound (EDTA) and metallic species, particularly copper and iron, species distribution diagrams were constructed using the software Make Equilibrium Diagrams Using Sophisticated Algorithms (MEDUSA) (Puigdomenech, 2004), and thermodynamic data reported in the National Institute of Standards and Technology (NIST) database were employed (National Institute of Standards and Technology (NIST), 2004).

3. Results and discussion

3.1. Chemical and thermodynamic analysis

3.1.1. Thermodynamics of the leaching process

According to the metallic composition of the LFP black mass (Table S1, supplementary material), the elements detected were iron (13.11±0.25wt%), phosphorus (8.04±0.16 wt%), copper (2.82±0.06 wt%), lithium (1.81±0.03 wt%), aluminum (1.21±0.04 wt%), nickel (0.32 ± 0.01 wt%), and cobalt (0.06±0.001 wt%).

Although representative amounts of iron, lithium, and phosphorus are present, the sample is not pure. These metallic impurities can affect leaching selectivity; however, some species (e.g., copper, aluminum, phosphorus, etc.) can benefit the leachates by serving as micronutrients (Hazra, 2016). Therefore, a thermodynamic analysis was conducted to determine the chemical behavior of the different metals that can be extracted and the specific leaching agents. For lithium extraction, sodium hydroxide was selected as the leaching agent, as it is a widely studied system. Several parameters have been examined, including concentrations ranging from 1 to 4 M and temperatures from 25 °C to over 90 °C. Additionally, different pretreatment and mechanochemical processes have been explored, achieving lithium leaching yields over 90%, and depending on the battery composition, other metals can also be extracted (Gaye et al., 2019; Wang et al., 2019; Pei et al., 2026).

According to Yang et al. (2024), the hydroxide is reduced during the leaching process, forming hydrogen (H_2) while sodium ions (Na^+) enter the LFP crystal structure, causing it to disintegrate. This fact contributes to the solubilization of lithium and phosphorus as Li^+ and PO_4^{3-}, and the formation of $Fe_3O_{4(s)}$, as illustrated in Eq. (2).

$$3LiFePO_{4(s)} + 6NaOH_{(aq)} \rightarrow 3Li^+ + 6Na^+ + 3PO_4^{3-} + Fe_3O_{4(s)} + 2H_2O_{(aq)} + H_{2(g)} \quad \Delta G^o = -237.27 kJ/mol \tag{2}$$

In the second leaching phase, EDTA was proposed to extract not only iron but also copper, which is present in the black mass sample (Table S1). EDTA is a chelating agent that forms stable complexes with most metal ions due to its ability to dissociate (Fig. 2a). These interactions result from a favorable combination of carboxylic groups, which facilitate salt formation, and amino groups, which create coordinate bonds. For this reason, EDTA is considered a strong sequestrant that keeps metal ions in aqueous solution (Flaschka, 1964; Wolf and Gilbert, 1992).

Fe-EDTA and Cu-EDTA complexes can act as micronutrients, especially when plants exhibit iron (chlorosis) or copper deficiency (Ma et al., 2019). In chelated fertilizers, EDTA forms stable complexes that prevent metal ions from reacting with other components, like carbonates, and stabilize solution pH (Liu et al., 2022). Conversely, these chelated fertilizers serve a specific purpose and are widely used to address metal deficiencies, particularly for foliar applications, in which the fertilizer is applied in small quantities (prepared from a concentrated solution, Table S3) and sprayed directly onto the leaves rather than applied to the soil (Basavaraj and Chetan, 2018; Liu et al., 2022).

The species distribution diagrams, Fig. 2b and 2c, show the stable species between EDTA and copper and iron ions (Cu^{2+}, Fe^{3+}, and Fe^{2+}). Thermodynamically, soluble species, metal-EDTA, are stable in both acidic and alkaline media, where the predominant soluble species are $Cu(EDTA)^{2-}$ (Log K at 25 °C = 20.57), $Cu(EDTA)OH^{3-}$ (Log K at 25 °C = 8.5), $Fe(EDTA)^-$ (Log K at 25 °C = 27.80), and $Fe(EDTA)^{2-}$ (Log K at 25 °C = 16.09) (Puigdomenech, 2004).

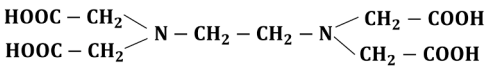
In fertilizer production, pH is crucial for stabilizing metal ions and facilitating the absorption of essential micronutrients by plants. Therefore, Fe-EDTA chelates must remain stable within a pH range of 4 to 6.5, whereas Cu-EDTA complexes are stable between pH 2 and 10 (Kasozi et al., 2019; Nouryon: Micronutrients-Product range and pH stability of chelated micronutrients, 2021). In mixed fertilizers, solutions that contain Cu-EDTA and Fe-EDTA chelates, a pH between 4 and 7.5 ensures appropriate stability (Hydro Fert: Fertilizers based on micronutrients, 2025). Based on this information, the pH range for the leaching tests in the EDTA system was delimited.

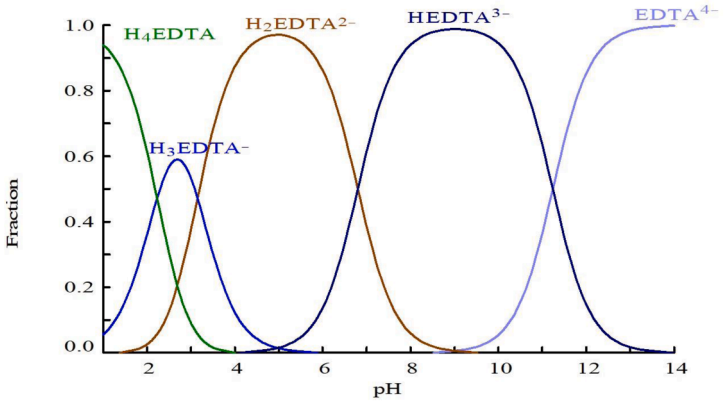
3.1.2. Thermodynamics of lithium recovery

To recover lithium from the leaching liquors, a chemical precipitation process is suggested. This method is one of the most traditional techniques for metal recovery. In this process, a chemical reagent is

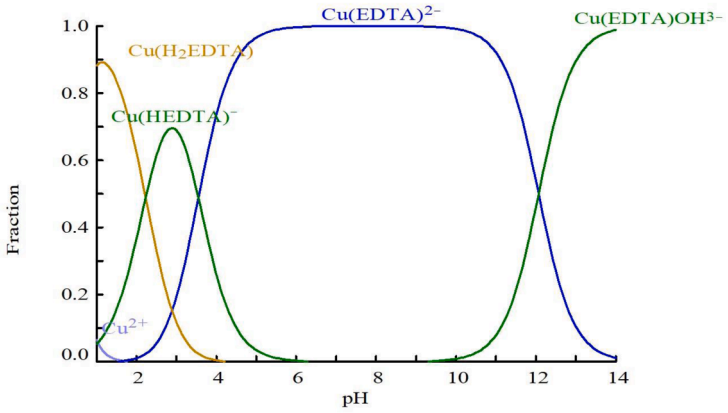
(a) EDTA dissociation

Ethylenediaminetetraacetic acid (EDTA):





(b) Cu-EDTA



(c) Fe-EDTA

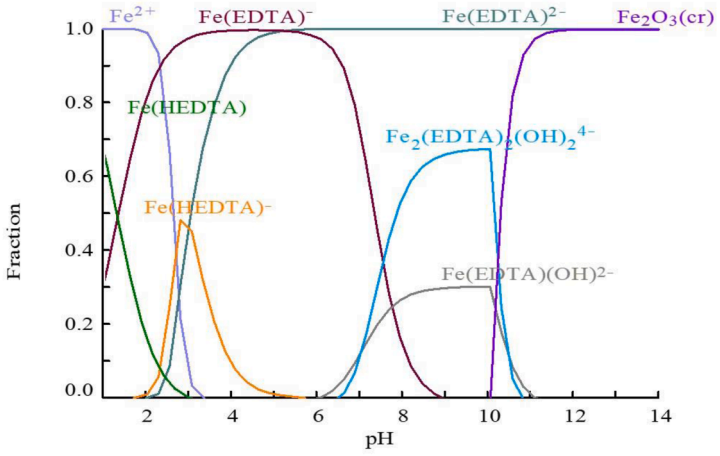


Fig. 2. Species distribution diagrams: (a) EDTA dissociation, (b) Cu-EDTA system, and (c) Fe-EDTA system.

added to the solution, facilitating the conversion of soluble ions into insoluble species by altering ionic equilibrium (Wang and Wu, 2017). In alkaline media, Li^+ and PO_4^{3-} can precipitated as $Li_3PO_{4(s)}$ (Log K (25°C) = − 10.63) according to the chemical reaction described in Eq. (3) (Dean, 1999; Xiao and Zeng, 2018).

$$3Li^+ + PO_4^{3-} \rightarrow Li_3PO_{4(s)} \quad \Delta G^o = -50\ kJ/mol \tag{3}$$

It has been demonstrated that lithium salt formation is enhanced within the pH range of 11 to 13 (Xiao and Zeng, 2018). Other studies (Mulwanda et al., 2021; Mendieta-George et al., 2022; Yang et al., 2024) indicate that raising the temperature from 45 °C to 90 °C also promotes the chemical reaction shown in Eq. (3), resulting in a high-purity product (~100%).

3.2. Lithium extraction and recovery

3.2.1. The effect of sodium hydroxide (NaOH) concentration on lithium extraction

The first stage of the process focused on lithium extraction and recovery. To extract lithium, sodium hydroxide (NaOH) was used as the leaching agent, a solid-liquid ratio of 20 g/L was employed, and the tests were performed at room temperature (25 °C). As shown in Fig. 3, the leaching yield of lithium and other extracted metals was analyzed as a function of time, considering different NaOH concentrations (1, 2, and 4 M). Lithium extraction was favorable with the three tested concentrations (Fig. 3a); its leaching yield was 98% (380 mg/L) after 60 min, particularly at 2 and 4 M NaOH. With the lower sodium hydroxide concentration (1 M NaOH), the leaching kinetics were slower than in the other systems, and the maximum extraction was 91%. Moreover, the three systems were distinguished by the fact that equilibrium was reached after 60 min of leaching.

Although lithium exhibited high dissolution, the system was not selective, as phosphorus and aluminum were also leached (Fig. 3b and 3c). The leaching efficiency of phosphorus was 97% (~1800 mg/L) when 1 and 2 M of NaOH were employed, and 91% (~1700 mg/L) with 4 M of NaOH. In this system, the extraction was almost complete within the first 30 min of leaching, then decreased to 91%. In contrast, at lower sodium hydroxide concentration, the extraction increased gradually to 91% (Fig. 3b).

On the other hand, the tendency of aluminum extraction was similar in the three systems (Fig. 3c). 96% (211 mg/L) of the aluminum was leached regardless of the sodium hydroxide concentration, and the leaching yields were ≥80% within the first 5 min (Fig. 3c). Despite phosphorus and aluminum dissolution, lithium extraction was achieved with acceptable yields. Also, it is important to highlight that the other metals present in the black mass sample, especially iron and copper, were not significantly leached; their leaching yields were ≤1%.

Based on the analysis of NaOH concentration, 2 M of the leaching agent and 60 min of leaching were sufficient to achieve maximum lithium dissolution, without adverse effects from other dissolved metals. In this alkaline system, it was crucial to analyze how the amount of black mass influences lithium extraction. For this reason, the solid-liquid ratio was modified, and its effect was studied.

3.2.2. The effect of the solid-liquid ratio in the alkaline system

The black mass sample was leached in 2 M NaOH at room temperature (25 °C) with solid-liquid ratios of 40, 60, 80, and 100 g/L. Lithium, phosphorus, and aluminum were the elements extracted (Fig. S1, supplementary material). Increasing the solid-liquid ratio did not improve lithium extraction, because the leaching yields after 60 min were ~80% (~1000 mg/L), 72% (1013 mg/L), and 65% (1038 mg/L) at 40, 60, 80, and 100 g/L, respectively (Fig. S1a). The leaching yield of phosphorus after 60 min was 87% (3577 mg/L) at 40 g/L, 76% (~4000 mg/L) at 60 g/L and 72% (~4100 mg/L) at 80 and 100 g/L (Fig. S1b), while aluminum was the only metal whose dissolution was enhanced with the increase of the solid-liquid ratio, 40 and 60 g/L: 79% (470 mg/L and 733 mg/L), 80 g/L and 100 g/L: 91% (~950 mg/L), after 60 min (Fig. S1c). Also, the leaching yields of lithium, phosphorus, and aluminum were lower than in the previous case with a solid-liquid ratio of 20 g/L (Fig. 3), where the results were ≥96%: 98% for lithium, 97% for phosphorus, and 96% for aluminum.

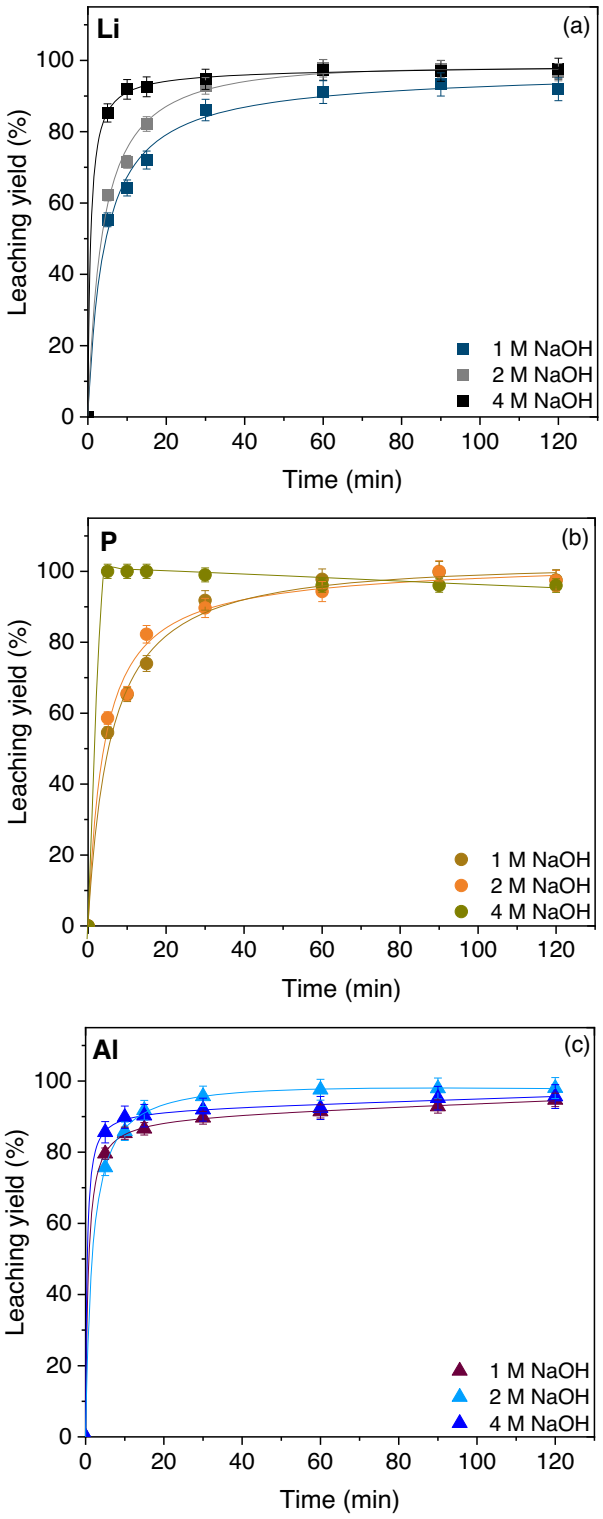


Fig. 3. Leaching yield of (a) Li, (b) P, and (c) Al, at different NaOH concentrations (1, 2, and 4 M), 20 g/L, room temperature (25 °C), and 300 rpm.

The favorable extraction of aluminum is attributed to the thermodynamic behavior between aluminum and sodium hydroxide. Aluminum is in the black mass as aluminum oxide, Al_2O_3, (Fig. S2), this species reacts in alkaline media according to Eq. (4) (Roine, 2006), and the formation of $Na[Al(OH)_4]_{(aq)}$ is thermodynamically possible.

$$Al_2O_{3(s)} + 2NaOH_{(s)} + 3H_2O_{(l)} \rightarrow 2Na[Al(OH)_4]_{(aq)} \quad \Delta G^o = -179 \ \ kJ/mol \tag{4}$$

The NaOH system faces solubility limitations when high amounts of solid are used, which are likely to affect mass transport (diffusion coefficients) and result in lower leaching efficiencies (Treybal, 1981). Another factor that directly affects metal dissolution is the concentration of the leaching agent (Faraji et al., 2022). To evaluate its effect on lithium leachability, additional experiments were conducted using 4 M NaOH and the previously tested solid-liquid ratios (as detailed in the supplementary material, Fig. S3). However, the leaching yields exhibited a similar tendency to those shown in Fig. S1, specifically for lithium and phosphorus. It has been demonstrated that when pH is over 10, lithium and phosphate ions can interact and co-precipitate (Yang et al., 2024). This fact can explain the behavior of both elements in the alkaline system. The results from these experiments, along with the data presented in Fig. S1, indicate that in a 2 M NaOH system operating at 25 °C, using 20 g of black mass per liter of solution for 60 min leads to almost complete dissolution of lithium (confirmed by analysis of the solid residue, Fig. S4), enabling recovery of lithium in a subsequent stage of the process.

3.2.3. Precipitation process for lithium recovery

Once the alkaline leaching was concluded, the PLS was heat-treated to recover lithium. In conventional precipitation, an additional reagent is used to form solid compounds with certain species. In contrast, this methodology supported the idea proposed by Yang et al. (2024), who determined that, in a solution rich in lithium and phosphate ions, the chemical reaction (Eq. (3)) occurs only when the temperature reaches ~90 °C for 2 h. Therefore, in this work, the leachates were heated at 90 °C. In this investigation, after 3 h, 60% of the leaching liquor (from the PLS with 98% Li, 380 mg/L; 97% P, 1793 mg/L; 96% Al, 211 mg/L) evaporated, and a white precipitate was formed (Fig. S5a). Subsequently, the dry solid was analyzed by XRD, and lithium phosphate ($Li_3PO_{4(s)}$) was the only compound detected (Fig. S5b). Additionally, the solid and the remaining solution were chemically analyzed, and it was determined that 60% (232 mg/L) of lithium precipitated and that the purity of the obtained salt was >98%, with only traces of aluminum as impurity. The elemental composition of the lithium salt was 16% Li and 25% P, corresponding to a lithium-to-phosphorus molar ratio of 2.82.

In this stage of the process, time and NaOH concentration are parameters that directly affect lithium precipitation. The sodium hydroxide concentration in the system must be lower than 4 M. At high leaching-agent concentrations, the excess NaOH promotes the coprecipitation of lithium and aluminum, favoring aluminum crystallization. For example, when precipitation tests were performed using leachates with 4 M NaOH (Fig. S6), a gel was formed, characteristic of aluminum hydroxide ($Al(OH)_3$) (Loh et al., 2000). The chemical analysis (Table S2) showed that aluminum indeed precipitated upon heat treatment of the solution. On the other hand, processing leachates with 2 M NaOH, 3 h was the optimal time to achieve the formation of $Li_3PO_{4(s)}$ with a negligible amount of aluminum. Increasing time did not guarantee the complete precipitation of phosphorus and, especially, lithium, which remained in the residual solution (Fig. S7). For complete recovery, further steps focusing on purification and a second precipitation are required.

3.3. Production of leachates rich in iron and copper for use in fertilizer production

3.3.1. Ethylenediaminetetraacetic acid (EDTA) for iron and copper dissolution: the influence of the leaching agent concentration and temperature on the dissolution of iron and copper

The solid residues from the alkaline treatment (2 M NaOH, 20 g/L, 60 min, at 25 °C) were leached with 0.1 M EDTA solutions to dissolve iron and copper; the leaching tests were also conducted at room temperature (25 °C). At room temperature, EDTA can dissociate and form soluble complexes with iron and copper over a wide pH range (Fig. 2), and given the metallic composition (Table S1), the proposed concentration is sufficient to promote metal dissolution. Fig. 4 shows metal leaching yields as a function of time. According to these results, iron and copper were preferably extracted (Fig. 4a), especially copper, whose leaching yield was ≥80% (≥ 350 mg/L) after 15 min and increased to 97% in the last two hours of leaching. In contrast, the iron leaching yield was ≤50% (≤1000 mg/L) throughout the process and remained constant after 90 min.

In this chemical system, the pH was analyzed. The initial pH value was ~4.5; upon completion of the leaching process, the measured pH was 5.6. Even though, in this pH range, soluble copper and iron complexes with EDTA can form (Fig. 2b and 2c), the chelating agent could not effectively coordinate iron (Fig. 4a). This is attributed to the amount of copper and iron in the original sample (Table S1). Thus, to achieve effective iron dissolution, the EDTA concentration and temperature were modified.

Two concentrations, 0.1 M and 0.3 M, were tested at 40 °C and 60 °C. These temperatures were selected to improve EDTA solubility in the aqueous medium (0.1 g/100 mL at 25 °C, Wolf and Gilbert, 1992). In this case, a high concentration of the leaching agent (0.3 M) guarantees enough EDTA ions (H_2EDTA^{2-}, Fig. 2a), and is also the maximum concentration that must be used in this chemical system because of the EDTA solubility limitation. Therefore, Fig. 4 also shows the leaching yield of the extracted metals with the two EDTA concentrations. The first system studied was 0.1 M at 40 °C (Fig. 4b), in which metal dissolution was favored, achieving leaching yields ≥80%. According to Fig. 4b, copper dissolution was higher than iron extraction during the first minutes of leaching and remained higher throughout the process; the leaching yields were 96% (400 mg/L) for copper and 79% (1500 mg/L) for iron.

When the EDTA concentration was increased to 0.3 M EDTA (Fig. 4c), iron dissolution improved compared to the previous system (0.1 M EDTA), and the maximum leaching yield was 97% (~1900 mg/L) after 90 min. After 120 min, its efficiency decreased, and the final leaching yield was 90% (1620 mg/L). On the other hand, copper extraction was constant, keeping a leaching yield of 96%. The tendency of copper and iron leaching yields, especially after 120 min, can be attributed to competition between metallic ions for coordination with EDTA. So, increasing the leaching agent concentration to 0.3 M, the optimal leaching time was 90 min (97% Fe and 96% Cu).

To determine the maximum iron and copper extraction, 0.3 M EDTA was used to ensure sufficient EDTA ions in solution. In this chemical system, the temperature was modified to 60 °C. Fig. 4d shows that the leaching yields of copper and iron were similar for the first 60 min; afterward, the leaching efficiency of iron remained constant at 96% (1932 mg/L). This means that adjusting the temperature improved iron leaching efficiency, but for copper, after 120 min, the leaching yield decreased, resulting in an extraction percentage of 90% (317 mg/L).

Based on the results shown in Fig. 4d, temperature enhanced the extraction of iron, the predominant metal in the black mass sample (Table S1). The leaching yield began to increase within the first minutes compared to the previous case (Fig. 4b and c), reaching equilibrium after 40 min. Copper was also favorably extracted, and a high leaching yield of ≥90% was achieved. Moreover, the pH of the EDTA solutions was also

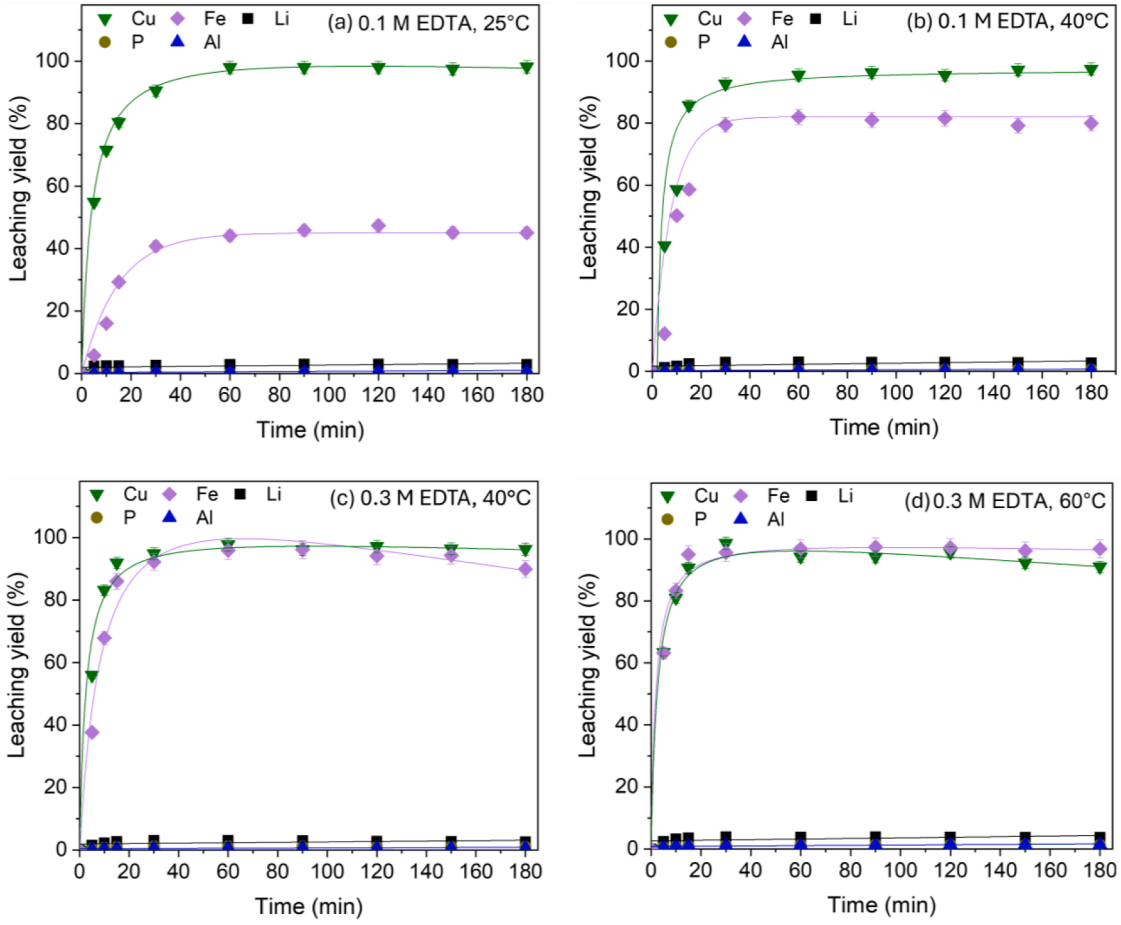


Fig. 4. Leaching yield. (a) 0.1 M EDTA at 25 °C, (b) 0.1 M EDTA at 40 °C, (c) 0.3 M EDTA at 40 °C, and (d) 0.3 M EDTA at 60 °C. All cases were at 300 rpm and using solid residue from the alkaline treatment (2 M NaOH, 20 g/L, 60 min, at 25 °C).

crucial. The pH of the solutions was not adjusted; in 0.1 M EDTA, the initial pH was ~4.5, and after the leaching process, the pH value was ~6, similar to the system which operated at room temperature (Fig. 4a). For 0.3 M EDTA, the pH changed from ~4.3 to pH 5. The pH range of the PLS is in accordance with the pH of commercial fertilizers, which must be between 4 and 7.5 to ensure the stability of copper and iron ions in EDTA solutions (Nouryon: Micronutrients-Product range and pH stability of chelated micronutrients, 2021). Therefore, at 0.3 M with an initial pH of ~4.3 at 60 °C, the leaching yields were 98% (1988 mg/L) Fe and ~96% (400 mg/L) Cu at 120 min, the time at which extraction of both metals reached its maximum.

The metal composition and pH of the leaching liquors were compared with a commercial mixed fertilizer and solutions from foliar applications, as shown in Table S3 (Hydro Fert: Fertilizers based on micronutrients, 2025; Growland: Fertilizer products, 2026; LeroChem: Iron sodium EDTA | Ferric chelate, 2026). According to Table S3, the concentrations of iron and copper in the leaching liquor are lower than those of the first product shown in Table S3. However, the amounts of copper and iron are within the range used for foliar applications; but it is important to note that the presence or absence of other species can influence micronutrient absorption (Verbeeck et al., 2020).

In the four chemical systems described previously (Fig. 4), not only copper and iron were leached, but also some traces of phosphorus, aluminum, and lithium. The leaching yields for phosphorus and aluminum were ≤0.6% (18 mg/kg P and 2 mg/kg Al), while ~2% (14 mg/kg) of lithium was extracted. It is well known that phosphorus and aluminum are also considered micronutrients and components of traditional (mineral) fertilizers, and their concentrations can reach 1591 mg/kg Al and 91 mg/kg P (Verbeeck et al., 2020). On the other hand, the benefits of lithium in plant growth are still under discussion and study. Nevertheless, it has been demonstrated that specific concentrations of this element can enhance the physiological development and enzymatic activity of certain plants; for example, in cereal grains (1–64 mg/kg), lettuce (7.5–22 mg/kg), and spinach (40 mg/kg) (Makus et al., 2006; Antonkiewicz et al., 2017; da Silva et al., 2019).

According to the information provided in this section, EDTA is a highly effective compound that achieves high base-metal leaching yields at low temperatures (<100 °C). Furthermore, under the tested conditions, no additional compounds, like oxidizing agents, are required in the chemical system. This results in leachates rich in iron and copper, which contain small amounts of additional compounds, and thus can be used for foliar applications. Fig. S7 shows the flowchart and mass balance of the whole process described in Sections 3.2 and 3.3.

Another aspect to consider in battery recycling is that batteries contain not only metals but also non-metallic substances. For example, the electrolyte consists of a conductive salt (e.g., lithium hexafluorophosphate $LiPF_6$) and carbonate-derived solvents (Zachmann et al., 2024). For that reason, in this study, the content of residual electrolyte solvents as well as their decomposition products and fluorinated compounds in the leaching solutions (for the optimal leaching systems), the original black mass sample, and the solid residues were investigated.

3.4. Analysis of impurities in naoh and EDTA leaching liquors

3.4.1. Decomposition of electrolyte solvents during the leaching process

The linear carbonates (e.g., dimethyl carbonate DMC, ethyl methyl carbonate EMC, diethyl carbonate DEC) are highly volatile,

inflammable, apolar liquids and contribute to the low viscosity of the electrolyte. In contrast, the cyclic carbonates (e.g., ethylene carbonate EC, propylene carbonate PC) exhibit much higher polarity and enable the conductive salt (e.g., lithium hexafluorophosphate $LiPF_6$) to dissolve in the solvent mixture (Xu, 2004).

As the first step of the analysis, the content of the electrolyte solvents in the black mass (original and untreated sample) was quantified using a hyphenation of gas chromatography and mass spectrometry (GC/MS). Only the cyclic carbonates, EC (28.01±1.88 mg/g) and PC (7.56 ±0.64 mg/g), were present in the black mass. In addition, low amounts of ethylene glycol and propylene glycol (EG, PG, <2 mg/g black mass) were detected. Both are common decomposition products of the cyclic carbonates. The more volatile linear electrolyte solvents (DMC, EMC, and DEC) evaporated already during the production of the black mass, which includes several (mechanical) pretreatment steps (Zachmann and Ebin, 2025).

Furthermore, the content of the electrolyte solvents on the solid residue from alkaline leaching, as well as in the NaOH and EDTA leaching liquors, was analyzed. GC/MS measurements of organic extracts revealed that neither on the solid leaching residue nor in either of the leaching solutions (NaOH and EDTA) were electrolyte solvents (EC, PC) or the corresponding decomposition products (EG, PG) present (Table 1, entry 1a-c). These observations suggest that the electrolyte solvents already decompose during the first alkaline leaching step, which was further investigated by suspending the black mass in different media (deionized water (Millipore Milli-Q), 2 M NaOH, 0.3 M EDTA). Subsequently, organic extracts of the resulting aqueous suspensions were analyzed via GC/MS as shown in Table 1 (entries 2, 3, and 4).

Independent of the treatment, the suspensions in water (Table 1, entry 2) contained electrolyte solvents (EC and PC), indicating no appreciable decomposition. Nevertheless, small amounts of ethylene and propylene glycol (EG, PG) were already present in the original black mass. However, the glycols were not detected via GC/MS because glycols are more soluble in water than in dichloromethane, which was used to extract a sample for GC/MS analysis.

In contrast, the electrolyte solvents decompose immediately in 2 M NaOH solution (Table 1, entry 3a) and thus could not be detected via GC/MS. As discussed before, the decomposition products (EG and PG) remain in the aqueous phase due to lower solubility in the organic solvent used for sample preparation. Furthermore, in 0.3 M EDTA solution, the electrolyte solvents are intact (Table 1, entry 4a) and were detected via GC/MS, even after treatment under leaching conditions (Table 1, entry 4b).

Table 1
GC/MS analysis of the leaching liquors, the solid residue from NaOH leaching, and suspensions of the black mass in different media. Detailed information on sample preparation is given in the experimental part. n.d. = not detected.

Entry	Composition	Treatment	Electrolyte solvents (EC, PC) Decomposition products (EG, PG)
1a	NaOH leaching liquor	-	n.d.
1b	Solid residue (from NaOH leaching)	-	n.d.
1c	EDTA leaching liquor	-	n.d.
2a	Black mass in	-	EC, PC
2b	water	1 h, 300 rpm at room temperature (25 °C)	EC, PC
3a	Black mass in 2 M	-	n.d.
3b	NaOH	1 h, 300 rpm at room temperature (25 °C)	n.d.
4a	Black mass in	-	EC, PC
4b	0.3 M EDTA	3 h, 300 rpm at 60 °C	EC, PC

Based on a study by Fu et al. (2016), where a mechanism for the hydrothermal conversion of ethylene carbonate (EC) to ethylene glycol (EG) is given, a mechanism for the decomposition of ethylene carbonate (EC) in alkaline media is proposed in Fig. S8. The mechanism suggests, in the first step, the nucleophilic attack of the carbonyl group by the hydroxide which triggers the ring opening of the cyclic carbonate (EC). After subsequent deprotonation, carbon dioxide is released, and the corresponding glycol (EG) is formed.

From Table 1 (entry 3) and the proposed chemical mechanism (Fig. S8), it can be concluded that the decomposition of electrolyte solvents occurred solely and completely during the alkaline leaching step in 2 M NaOH. Moreover, during the GC/MS sample preparation for the analysis of the solid leaching residue, no water is involved. Therefore, if present, residual glycols (EG, PG) can be detected in the solid leaching residue, which is further used for the final acidic leaching step with EDTA. However, entry 1b (Table 1) clearly states that no decomposition products (EG, PG) are present on the solid leaching residue and therefore remain in the alkaline leaching solution. Hence, the EDTA solution does not contain electrolyte solvents (EC, PC) or decomposition products (EG, PG).

3.4.2. *Fluoride ion (F^-) content in naoh and EDTA liquors*

Fluoride is a typical component of batteries because it constitutes the electrolyte, binder, and the solid electrolyte interface components (Gopinadh et al., 2022). However, in battery recycling, fluoride ion (F^-) is cataloged as an impurity because it can affect the production or purity of recycled materials (Jiang et al., 2025). For that reason, in this work, the fluoride content was analyzed in the leaching liquors of both chemical systems, alkaline and acid leaching, using an Ion-Selective Electrode (ISE). Table 2 shows the concentration of fluoride ions in the NaOH and EDTA liquors (optimal experimental conditions).

According to Table 2, 628 ppm of fluoride was detected in alkaline solutions, whereas in EDTA leaching liquors, it was 3.5 ppm. In chelated fertilizers, there is no evidence of fluoride presence, however, in soil, the fluoride content is in a range of 150–400 ppm, and in clay soil the amount of 1000–3500 ppm (Hong et al., 2016; Fuge, 2019). Therefore, the detected fluoride in the EDTA leachates is negligible compared to the natural soils, which means that the PLS rich in iron and copper are free of potential impurities.

4. Conclusions

This work proposed a methodology to produce iron- and copper-enriched solutions from spent LFP batteries potentially used in fertilizer production, suitable for foliar applications. Moreover, a secondary and profitable product was obtained, lithium phosphate ($Li_3PO_{4(s)}$), which can be used as a chemical precursor for producing new batteries. The method employed a hydrometallurgical process divided into two stages. The first one, performed in alkaline media, used 2 M NaOH, 20 g of black mass per liter of solution, 60 min, 300 rpm at 25 °C, and allowed 98% lithium extraction. Subsequently, through heat treatment (90 °C for 3 h), lithium phosphate salt with a purity of >98% was obtained. It was demonstrated that to achieve selective precipitation of lithium and phosphate ions, the maximum concentration of NaOH in the leaching solutions must be 2 M. At higher concentrations, the coprecipitation of aluminum, another metal dissolved in NaOH solutions, is favored,

Table 2
Fluoride concentration in NaOH and EDTA leachates.

Leaching system	Experimental conditions	Concentration of fluoride ion (ppm)
NaOH	2 M NaOH, 20 g/L, 60 min, and room temperature (25 °C).	682 ± 0.25
EDTA	0.3 M EDTA, 60 °C, 300 rpm, using the solid residue from the alkaline treatment.	3.5 ± 0.13

thereby preventing the formation of the lithium phosphate salt.

To treat the solid residues from the first leaching stage, ethylenediaminetetraacetic acid (EDTA) was used to dissolve iron and copper. This leaching agent achieved near-complete dissolution of both metals (98% Fe and ~96% Cu) using 0.3 M EDTA at 60 °C, 300 rpm for 120 min. In this system, raising the temperature increased EDTA solubility in aqueous media and also contributed to base-metal extraction. On the other hand, the pH value (between ~4.3 and 5) of the iron and copper solutions is comparable to that of commercial fertilizers, which guarantees the stabilization of the metal ions in EDTA solutions. However, the concentration of base metals was lower than that of some commercial products. Therefore, future studies could assess formulations comparable to commercially available fertilizers or foliar solutions.

Furthermore, the leaching liquors were analyzed to detect impurities like electrolyte solvents and fluoride. Techniques such as Gas Chromatography Mass Spectrometry and the fluoride-selective electrode confirmed the negligible presence of impurities, ensuring the products were uncontaminated. Finally, one notable feature of the proposed methodology is that no additional reagents, such as oxidizing agents, were used, and that high temperatures were avoided, thereby ensuring a viable and promising process for manufacturing agricultural products.

CRediT authorship contribution statement

Brenda Segura-Bailón: Writing – original draft, Visualization, Validation, Software, Methodology, Investigation, Formal analysis, Data curation, Conceptualization. **Philipp Mikšovsky:** Writing – original draft, Visualization, Validation, Methodology, Formal analysis. **Burçak Ebin:** Writing – review & editing, Supervision, Resources, Funding acquisition. **Martina Petranikova:** Writing – review & editing, Supervision, Resources, Project administration, Funding acquisition, Conceptualization.

Declaration of competing interest

The authors declare that they have no known competing financial interests or personal relationships that could have appeared to influence the work reported in this paper.

Acknowledgements

The authors thank Stena Recycling International AB for financial support and for providing the black mass sample, as well as BASE (Batteries Sweden) by VINNOVA (Grant number: 2024–03853). Finally, the authors thank the Chalmers Materials Analysis Laboratory (CMAL) for providing access and support to perform materials characterization.

Supplementary materials

Supplementary material associated with this article can be found, in the online version, at doi:10.1016/j.resconrec.2026.109219.

Data availability

Data will be made available on request.

References

Alzate-Zuluaga, M.Y., Cardarelli, M., Rouphael, Y., Cesco, S., Pii, Y., Colla, G., 2023. Iron nutrition in agriculture: from synthetic chelates to biochelates. Sci. Hortic. 312, 111833. https://doi.org/10.1016/j.scienta.2023.111833.

Anka, H., Taskin, M.B., Gunes, A., Inal, A., 2024. The effect of phosphorus fertilizer under the influence of iron and zinc treatments on nutrient content and lettuce yield. J. Plant Nutr. 47, 750–761. https://doi.org/10.1080/01904167.2023.2280130.

Antonkiewicz, J., Jasiewicz, C., Koncewicz-Baran, M., Baczek-Kwinta, R., 2017. Determination of lithium bioretention by maize under hydroponic conditions. Arch. Environ. Prot. 43, 94–104. https://doi.org/10.1515/aep-2017-0036.

Barragán-Mantilla, S.P., Ortiz, R., Almendros, P., Sánchez-Martín, L., Gascó, G., Méndez, A., 2024. Advances in the sustainable production of fertilizers from spent Zinc-based batteries. Sustainability 16, 4255. https://doi.org/10.3390/su16104255.

Basavaraj, P., Chetan, H.T., 2018. Foliar fertilization of nutrients. Marumegh 3, 49–53.

da Silva, R.R., de Faria, A.J.G., Alexandrino, G.d.C., Ribeiro, E.A., dos Santos, A.C.M., Deusdara, T.T., do Nascimento, I.R., Nascimento, V.L., 2019. Enrichment of lithium in lettuce plants through agronomic biofortification. J. Plant. Nutr. 42, 2102–2113. https://doi.org/10.1080/01904167.2019.1648671.

Dean, J.A., 1999. Lange's Handbook of Chemistry. McGraw-Hill, Inc., New York fifteenth ed.

European Commission: Sustainable agriculture in the EU, 2025. https://agriculture.ec.europa.eu/cap-my-country/sustainability_en (accessed 25 June 2025).

Faraji, F., Alizadeh, A., Rashchi, F., Mostoufi, N., 2022. Kinetics of leaching: a review. Rev. Chem. Eng. 38, 113–148. https://doi.org/10.1515/revce-2019-0073.

Fazilova, M., Hasanov, S., Alimo, U., Raxmanova, M., Sadullaev, S., 2023. Study of microelement containing nitrogen fertilizers based on spent lithium-ion battery. Conf. Sr.: Earth Environ. Sci. 1142, 012047. https://doi.org/10.1088/1755-1315/1142/1/012047.

Flaschka, H.A., 1964. EDTA Tritations: An Introduction to Theory and Practice. Pergamon Press, London second ed.

Fortune Business Insights: Lithium Iron Phosphate Battery Market Size, Share & Industry Analysis, 2025. By Type (Portable Battery, Stationary Battery), By Application (Automotive, Industrial, Energy Storage System, Consumer Electronics, and Others), and Regional Forecast, 2026-2034. https://www.fortunebusinessinsights.com/lithium-ion-li-ion-phosphate-batteries-market-102152 (accessed 20 November 2025).

Fu, J., Jiang, N., Ren, D., Song, Z., Li, L., Huo, Z., 2016. Hydrothermal conversion of ethylene carbonate to ethylene glycol. Int. J. Hydrog. Energy 41, 9118–9122. https://doi.org/10.1016/j.ijhydene.2015.12.083.

Fuge, R., 2019. Fluorine in the environment, a review of its sources and geochemistry. Appl. Geochem. 100, 393–406. https://doi.org/10.1016/j.apgeochem.2018.12.016.

Gaye, N., Gueye, S.G., Ledauphi, L., Blade, M., Seck, M., Wele, A., Diaw, M., 2019. Alkaline leaching of metals from cathodic materials of spent lithium-ion batteries. Asian J. Appl. Chem. Res. 3 (2), 1–7. https://doi.org/10.9734/ajcr/2019/v3i230088.

Gehlot, P., Yadav, J., Chittora, D., Meena, S.J., Meena, P., Jain, T., 2024. Biofertilizers, bionanofertilizers and nanofertilizers: ecofriendly alternatives for crop production. J. Mycopathol. Res. 62 (2), 241–259. https://doi.org/10.57023/JMycR.62.2.2024.241.

Gopinadh, S.V., Phanendra, V.R.L., John, B., Mercy, T.D., 2022. Fluoride-ion batteries: state-of-the-art and future perspectives. SM&T 32, e00436. https://doi.org/10.1016/j.susmat.2022.e00436.

Growland: Fertilizer products, 2026. https://www.growland.se/CANNA-MONO-Iron-1L?gad_source=1&gad_campaignid=17338327397&gbraid=0AAAADoddOVVyMEprb1kdA7YT2bMCHXfx&gclid=Cj0KCQjwguLSBhDLARIsAH-yPrGHzRbEA6n8qjHlxqSeTy9RkZEe6nWbkUWdlYWHSTIa7pp7o98snXoaAq9lEALw_wcB (accessed 16 July 2026).

Hazra, G., 2016. Different types of eco-friendly fertilizers: an overview. Sustain. Environ. 1, 54. http://www.scholink.org/ojs/index.php/se.

Hong, B.D., Joo, R.N., Lee, K.S., Lee, D.S., Rhie, J.H., Min, S., Song, S.G., Chung, D.Y., 2016. Fluoride in soil and plant. Korean J. Agric. Sci. 43 (4), 522–536. https://doi.org/10.7744/kjoas.20160054.

Hydro Fert: Fertilizers based on micronutrients, 2025. https://hydrofert.it/wp-content/uploads/2024/02/Micrap-Rame.pdf (accessed 22 April 2025).

Jiang, Y., Peng, C., Zhou, K., Zhou, H., Chen, T., Zhang, G., Chen, W., 2025. Impact and removal of fluorine impurity in the comprehensive recovery of spent $LiFePO_4$/C. Sep. Purif. Technol. 362, 131766. https://doi.org/10.1016/j.seppur.2025.131766.

Kasozi, N., Tandlich, R., Fick, M., Kaiser, H., Wilhelmi, B., 2019. Iron supplementation and management in aquaponic systems: a review. Aquac. Rep. 15, 100221. https://doi.org/10.1016/j.aqrep.2019.100221.

LeroChem: Iron sodium EDTA | Ferric chelate, 2026. https://lerochem.eu/en/pagrindinis/427-ironedta99fe13kg.html?srsltid=AfmBOophMCf6OH4iLsgnOkggcj524y3CwEiFFaJOG4_0TO28zViaPD6 (accessed 14 July 2026).

Li, P., Luo, S., Zhang, L., Wang, Y., Lin, Y., Xu, C., Guo, J., Cheali, P., Xia, X., 2024. Progress, challenges, and prospects of spent lithium-ion batteries recycling: a review. J. Energy Chem. 89, 144–171. https://doi.org/10.1016/j.jechem.2023.10.012.

Liu, G., Hanlon, E., Li, Y., 2022. Understanding and Applying Chelated Fertilizers Effectively Based on Soil pH. IFAS Extension University of Florida. https://growables.org/information/documents/ChelatedFertilizers.pdf (accessed 16 January 2026).

Loh, J.S.C., Fogg, A.M., Watling, H.R., Parkinson, G.M., O'Hare, D., 2000. A kinetic investigation of gibbsite precipitation using in situ time resolved energy dispersive X-ray diffraction. Phys. Chem. Chem. Phys. 2, 3597–3604. https://doi.org/10.1039/b00305n.

Luo, B., Yan, Q., Zhou, Y., Dong, Z., Huang, X., Zhao, Z., 2025. Advances and challenges in recycling spent $LiFePO_4$ batteries. Se. Purif. Technol. 362, 131780. https://doi.org/10.1016/j.seppur.2025.131780.

Ma, J., Zhang, M., Liu, Z., Chen, H., Li, Y., Sun, Y., Ma, Q., Zhao, C., 2019. Effects of foliar application of the mixtures of copper and chelated iron on the yield, quality, photosynthesis, and microelement concentration of table grape (Vitis vinifera L.). Sci. Hortic. 254, 106–115. https://doi.org/10.1016/j.scienta.2019.04.075.

Makus, D.J., Zibilske, L., Lester, G., 2006. Effect of light intensity, soil, type, and lithium addition on spinach and mustard greens leaf constituents. Subtrop. Plant Sci. 58, 35–41.

Markets and markets: Fertilizers Market by Type (Chemical Fertilizers and Biofertilizers), 2025. Crop type (Cereals & Grains, Oilseeds & Pulses, Fruits & Vegetables), mode of application (Soil, Foliar, Fertigation), and region-global forecast to 2023. htt

ps://www.marketsandmarkets.com/Market-Reports/fertilizers-market-114997228.html (accessed 5 May 2025).
Mendieta-George, D., Pérez-Garibay, R., Solís-Rodríguez, R., Fuentes-Aceituno, J.C., Alvarado-Gómez, A., 2022. Study of the direct production of lithium phosphate with pure synthetic solutions and membrane electrolysis. Miner. Eng. 185, 107713. https://doi.org/10.1016/j.mineng.2022.107713.
Mulwanda, J., Senanayake, G., Oskierski, H., Altarawneh, M., Dlugogorski, B.Z., 2021. Leaching of lepidolite and recovery of lithium hydroxide from purified alkaline pressure leach liquor by phosphate precipitation and lime addition. Hydrometallurgy 201, 105538. https://doi.org/10.1016/j.hydromet.2020.105538.
National Institute of Standards and Technology (NIST), 2004. Database 46.8, critically selected stability constants of metal complexes. V8.
Nouryon: Micronutrients-Product range and pH stability of chelated micronutrients, 2021. https://www.nouryon.com/globalassets/inriver/resources/brochure-micronutrients-product-range-global-en.pdf (accessed 2 February 2026).
Passalacqua, J., 2023. The role of phosphates in the LFP battery supply chain. In: IFA: International Fertilizer Association: Global Markets Conference. https://firstphosphate.com/23-07-12%20IFA_GlobalMarketsConference.pdf (accessed 10 January 2026).
Pei, Y., Zhao, Q., Liu, L., Yang, J., Zhang, S., Zhang, X., 2026. Mechanistic insights into NaOH-driven crystal destruction and selective lithium extraction from spent LiFePO4 via mechanochemistry. Waste Manag 222, 115649. https://doi.org/10.1016/j.wasman.2026.115649.
Puigdomenech, I., 2004. Make equilibrium diagrams using sophisticated algorithms (MEDUSA). Inorganic Chemistry. Royal Institute of Technology. v1. https://sites.google.com/site/chemdiagr/ (accessed 25 September 2025).
Quitzow, R., Balmaceda, M., Goldthau, A., 2025. The nexus of geopolitics, decarbonization, and food security gives rise to distinct challenges across fertilizer supply chains. One Earth 8, 101173. https://doi.org/10.1016/j.oneear.2024.12.009.
ReNutrients, 2025. How safe are alkaline batteries as raw material for fertilisers? https://www.renutrients.com.au/howsafeiszmgrow#:~:text=To%20make%20alkaline%20batteries%20into,used%20directly%20for%20soil%20fertilization (accessed 13 December 2025).
Roine, A., 2006. HSC Chemistry: chemical reaction and equilibrium software with an extensive thermochemical database. Metso Finland Oy v6. https://www.hsc-chemistry.com.
Treybal, R.E., 1981. Mass-Transfer Operations. McGraw-Hill Inc., Singapore third ed.
Verbeeck, M., Salaets, P., Smolders, E., 2020. Trace element concentrations in mineral phosphate fertilizers used in Europe: a balanced survey. Sci. Total Environ. 712, 136419. https://doi.org/10.1016/j.scitotenv.2019.136419.
Wang, W., Wu, Y., 2017. An overview of recycling and treatment of spent $LiFePO_4$ batteries in China. Resour. Conserv. Recycl. 127, 233–243. https://doi.org/10.1016/j.resconrec.2017.08.019.
Wang, W., Zhang, X., Liu, S., 2019. A simplified process for recovery of Li and Co from spent $LiCoO_2$ cathode using Al foil as the in situ reductant. ACS Sustain. Chem. Eng. 7, 12222–12230. https://doi.org/10.1021/acssuschemeng.9b01564.
Wang, X., Gaustad, G., Babbitt, C.W., 2016. Targeting high value metals in lithium-ion battery recycling via shredding and size-based separation. Waste Manag 51, 204–213. https://doi.org/10.1016/j.wasman.2015.10.026, 240-213.
Wolf, P., Gilbert, A., 1992. EDTA-ethylenediaminetetraacetic acid. In: Hutzinger, O. (Ed.), The Handbook of Environmental Chemistry. Springer-Verlag Berlin Heidelberg, New York, pp. 243–258.
Xiao, C., Zeng, L., 2018. Thermodynamic study on recovery of lithium using phosphate precipitation method. Hydrometallurgy 178, 283–286. https://doi.org/10.1016/j.hydromet.2018.05.001.
Xu, K., 2004. Nonaqueous liquid electrolytes for lithium-based rechargeable batteries. Chem. Rev. 104, 4303–4418. https://doi.org/10.1021/cr030203g.
Yang, W., Liu, X., Zhou, X., Tang, J., Su, F., Li, Z., Yang, J., Ma, Y., 2024. Mechanism of selective lithium extraction from spent $LiFePO_4$ cathodes in oxidizing alkaline leaching system. Se. Purif. Technol. 329, 125237. https://doi.org/10.1016/j.seppur.2023.125237.
Yue, X.H., Zhang, C.C., Zhang, W.B, Wang, Y., Zhang, F.S., 2021. Recycling phosphorus from spent $LiFePO_4$ battery for multifunctional slow-release fertilizers preparation and simultaneous recovery of lithium. Chem. Eng. J. 426, 131311. https://doi.org/10.1016/j.cej.2021.131311.
Zachmann, N., Ebin, B., 2025. Supercritical CO_2 extraction behavior of electrolyte solvents from Li-ion battery black mass. J. CO2 Util. 99, 103145. https://doi.org/10.1016/j.jcou.2025.103145.
Zachmann, N., Fox, R.V., Petranikova, M., Ebin, B., 2024. Implementation of a sub-and supercritical carbon dioxide process for the selective recycling of the electrolyte from spent Li-ion battery. J. CO2 Util. 81, 102703. https://doi.org/10.1016/j.jcou.2024.102703.
Zhang, X., Liu, Z., Qu, D., 2023. Proof-of-concept study of ion-exchange method for recycling of $LiFePO_4$ cathode. Waste Manag 157, 1–7. https://doi.org/10.1016/j.wasman.2022.12.003.
Zhao, T., Mahandra, H., Marthi, R., Ji, X., Zhao, W., Chae, S., Traversy, M., Li, W., Yu, F., Li, L., Choi, Y., Ghahreman, A., Zhao, Z., Zhang, C., Kang, Y., Lei, Y., Song, Y., 2024. An overview on the life cycle of lithium iron phosphate: synthesis, modification, application, and recycling. Chem. Eng. J. 485, 149923. https://doi.org/10.1016/j.cej.2024.149923.
Zhou, H., Li, W., Poulet, T., Basarir, H., Karrech, A., 2024. Life cycle assessment of recycling lithium-ion battery related mineral processing by-products: a review. Miner. Eng. 208, 108600. https://doi.org/10.1016/j.mineng.2024.108600.
Zulfiqar, F., Navarro, M., Ashraf, M., Akram, N.A., Munné-Bosch, S., 2019. Nanofertilizer use for sustainable agriculture: advantages and limitations. Plant Sci. J. 289, 110270. https://doi.org/10.1016/j.plantsci.2019.110270.